Mimetic butterfly wings through mimetic butterfly eyes: Evidence that brightness vision helps *Adelpha fessonia* identify potential mates

Andrew Dang[1], Gary D. Bernard[2], Furong Yuan[1,3], Aide Macias-Muñoz[1,4], Ryan I. Hill[5], J. P. Lawrence[1,6], Aline G. Rangel Olguin[1,7,8], Armando Luis-Martínez[9], Sean P. Mullen[10], Jorge Llorente-Bousquets[9], Adriana D. Briscoe[1]

[1]Department of Ecology and Evolutionary Biology, University of California, Irvine, CA

[2]Department of Electrical & Computer Engineering, University of Washington, Seattle, WA

[3]Department of Process Development, Lonza Houston Inc, Houston, TX

[4]Department of Ecology and Evolutionary Biology, University of California, Santa Cruz, CA

[5]Department of Biological Sciences, University of the Pacific, Stockton, CA

[6]Lyman Briggs College, Michigan State University, East Lansing, MI

[7]Centro de Ciencias Genómicas, Universidad Nacional Autónoma de México, Mexico

[8]Department of Physiology, McGill University, Canada

[9]Museo de Zoología, Departamento de Biología Evolutiva, Facultad de Ciencias, Universidad Nacional Autónoma de México, Ciudad de México, Mexico

[10]Department of Biology, Boston University, Boston, MA

Abstract

Müllerian mimicry arises when conspicuous unprofitable species share a color pattern, gaining protection because predators learn and avoid the warning colors of a bad meal. Coloration also has other functions. For example, how does one butterfly recognize another of the same species to mate? Color vision is thought to play a key role in driving the evolution of animal color patterns via natural or sexual selection, while achromatic (brightness) vision is often ignored as a possible mechanism for species recognition. Here we find evidence that brightness vision rather than color vision helps some mimetic *Adelpha* butterflies identify potential mates while their co-mimetic wing coloration is indiscriminable to avian predators. To do so, we examined the visual system of the butterfly *Adelpha fessonia,* a member of a diverse genus of butterflies comprising over 200 taxa with multiple mimicry complexes. We characterized the photoreceptors of *A. fessonia* using RNA-seq, eyeshine, epi-microspectrophotometry, optophysiology and comparative sequence analysis. We used these data to model the discriminability of wing color patches of *A. fessonia* in relation to those of its sympatric co-mimic, *A. basiloides*, through *A. fessonia* and avian visual systems. Adult *A. fessonia* eyes express three visual opsin mRNAs encoding long wavelength-, blue-, and ultraviolet-sensitive rhodopsins with peak sensitivities (λ_{max} values) at 530 nm, ~431 nm and 355 nm, respectively. Red-reflecting ommatidia, found in other nymphalid butterflies such as monarchs and *Heliconius* butterflies, are absent from the eyeshine of *A. fessonia*, indicating *A. fessonia* eyes lack heterogeneously expressed red filtering pigments and red-sensitive photoreceptors. Visual models of *Adelpha* wing coloration suggests that *A. fessonia* can distinguish conspecifics from co-mimics using achromatic vision. Avian predators, on the other hand, cannot distinguish between co-mimic wing color using either chromatic or achromatic cues. Taken together, these results suggest that mimetic wing color patterns and visual systems have evolved in tandem to maintain mimicry while avoiding mating between look-alike species.

Introduction

Müllerian mimicry is an effective defensive strategy against predators where multiple unprofitable species adopt the same conspicuous appearance and contribute to predators avoiding the conspicuous signal. These defenses include but are not limited to chemical, physiological, and behavioral defenses. *Limenitis* butterflies provide several examples of such a phenomenon with some species mimicking other defended species. For instance, *L. archippus* (viceroy) benefits from the defenses of its co-mimics, *Danaus plexippus* (monarch) and *D. gillippus* (queen), as avian predators learn to associate distastefulness with the similar wing patterns of both species (Prudic et al. 2007, 2019). Though mimicry can involve other sensory modalities such as auditory mimicry in moths (O'Reilly et al. 2019), most studies of mimicry emphasize coloration and vision.

Studies of mimicry have generally focused on the targeting of prey by predators (Rowland et al. 2007; Thurman and Seymoure 2015; McClure et al. 2019). Examples include avian predators learning to avoid brightly colored frogs (Darst and Cummings 2006) and aposematic butterflies (Chai et al. 1986; Prudic et al. 2002; Finkbeiner et al. 2018), and carnivores learning to avoid mimetic snakes (Pfennig et al. 2001). However, the perceptual capabilities of prey and predator considered jointly have only been investigated relatively recently (Bybee et al. 2012; Llaurens et al. 2014; Dalbosco Dell'Aglio et al. 2018). For most birds, moth and butterfly larvae and adults comprise a key component of their diet, and lepidopteran abundance is positively correlated with bird reproductive success (Nell et al. 2023). Despite these studies, there is still a dearth in knowledge of the visual systems of lepidopteran prey and how these systems contribute to the evolution and maintenance of butterfly aposematism and mimicry.

This study focuses on the visual system of *Adelpha fessonia*, a member of a genus, which contains many species with a white stripe on their wings. The genus *Adelpha* consists of over 100 described species and a similar number (~100) of subspecies (Willmott 2003a) ranging from the southern United States to South America. Moreover, recent phylogenies suggest that *Limenitis* (Ebel et al. 2015) and the Asian genus *Athyma* (Wu et al. 2019) should also be included in *Adelpha*. Among *Adelpha* adults, wing patterns involve multiple convergent wing coloration patterns suggesting multiple mimicry complexes (Willmott 2003a). For example, at least seven *Adelpha* species in Venezuela have independently evolved an orange band bordering on and touching the white band of the dorsal hindwing (Willmott 2003a). A study in Costa Rica and Ecuador deploying clay model butterflies and counting bird attacks found that mimetic *Adelpha* wing color patterns are an effective defense mechanism against predators (Finkbeiner et al. 2018). This study and others (Finkbeiner et al. 2017) have highlighted the frequency-dependent benefits conferred on the mimic by the model and have also revealed some nuances in the classification of a butterfly species as either model or mimic. A study of natural populations of the model *Danaus gilippus* (queen) butterfly and its mimic *L. archippus* (viceroy) in Florida found that unpalatability of the mimic increases where the model is rare, transforming both species in those geographical localities into co-mimics (Prudic et al. 2019).

Our focal taxon, *Adelpha fessonia fessonia,* can be found near streams from Panama to Mexico, and occasionally in the lower Rio Grande Valley in Texas (Willmott 2003a). *Adelpha fessonia fessonia* (hereafter just *A. fessonia*) has orange forewing tips, with conspicuous white bands on both wings (Fig. 1A) that likely act to reduce predation

in multiple ways: by signaling escape potential, by signaling unpalatability and/or by disrupting prey recognition (Fig. 1 A,B; Stobbe and Schaefer, 2008). The white stripe also likely influences mating success (Lederer 1960). Like other *Adelpha* butterflies, *A. fessonia* fly in a quick and unpredictable manner, likely causing predators to expend more energy in catching the prey than obtaining them, thus associating butterflies with similar patterns as being too costly to bother catching (Gibson 1974; Mallet and Singer 1987; Páez et al. 2021). *Adelpha fessonia* may be distasteful, obtaining toxins from the plants that they consume as larvae. While there is a diversity of larval host plants used by species in the genus, *A. fessonia* consumes Rubiaceae plants in the genus *Randia* as larvae (Willmott 2003a). Adults may also maintain unpalatability by feeding on white *Cordia* flowers, which are Boraginaceae plants that are hypothesized to contribute to the distastefulness of unpalatable *Adelpha* species (Hill and Mullen 2019). Across the genus, larval host plant diversity is correlated with increasing *Adelpha* species diversity, suggesting an evolutionary arms race between *Adelpha* butterflies and their host plants (Ebel et al. 2015; Mullen et al. 2011).

Although many species of *Adelpha* share the general orange-tip and white band appearance, *Adelpha fessonia* is unique in having the white stripe continuously unbroken from the costa to the anal margin (Willmott 2003a). A second species, *A. basiloides*, is similar in having some white expanding into the discal cell, with a small break in the white stripes differentiating the two. These species share common localities in the United States, Mexico (e.g., Luis-Martínez et al. 2022), Guatemala, Belize, El Salvador, Honduras, Nicaragua, Costa Rica, and Panama (Willmott 2003a) which, combined with their similar wing patterns, suggests they are mimics of each other. Their

shared color pattern may lead to generalization from predators to avoid unprofitable prey. Strengthening the case for mimicry is that in Central America *A. basiloides* white band is wide, matching *A. fessonia* and other taxa, but in western Ecuador, *A. basiloides* white band is narrow, matching several other *Adelpha* species present there (Willmott 2003a).

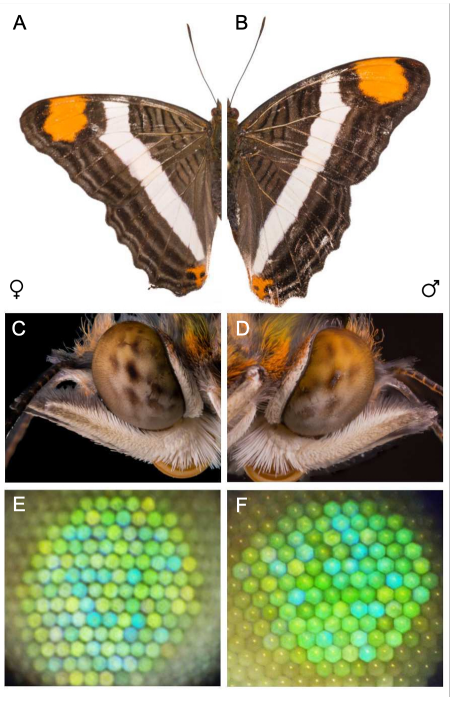

Figure 1. *Adelpha fessonia* wings, compound eyes, and eyeshine. Photographs of a female (left column) and male (right column) *Adelpha fessonia* wings (A and B), eyes (C and D) and eyeshine (E and F).

For many butterflies in the family Nymphalidae, which includes the *Adelpha/Limenitis* genera, vision is based on three opsin-based photoreceptors (Frentiu et al. 2007a,b; Pohl et al. 2009). This is commonly found in flower foraging insects as seen in honeybees (Peitsch et al. 1992), bumblebees (Spaethe and Briscoe 2005), and hawkmoths (White 2003). Typically, these photopigments are encoded by two short wave-sensitive opsin genes (*UVRh* and *BRh*) and one long wave-sensitive (*LWRh*)

opsin gene (Briscoe 2008; Briscoe and Chittka 2001) although exceptions exist (Mulhair et al. 2023; Kuwalekar et al. 2022; Sondhi et al. 2021). Opsin proteins together with a light-absorbing 11-*cis*-*3*-hydroxy retinal chromophore are the constituent parts of photoreceptor molecules that are sensitive to particular wavelengths of light. Amino acid substitutions in the chromophore binding pocket domain of the opsin protein can spectrally tune the wavelength of peak absorbance (λ_{max}) of the photopigment (Wakakuwa et al. 2010). Additional photoreceptor classes can also be produced via opsin gene duplication or from single opsins expressed together with photostable filtering pigments that coat the rhabdom (Arikawa et al. 2009).

Lepidoptera rely on vision to navigate and interact with their world. *Adelpha fessonia* is no exception. However, little is known about how the visual system of *Adelpha* butterflies affects their ability to detect potential mates whilst living in habitats shared by communities of co-mimics. A PCR-based survey of opsins expressed in adult eyes of *L. arthemis astyanax* and *L. archippus* yielded three opsin mRNA transcripts, encoding ultraviolet (UV)-sensitive, blue-sensitive and long wavelength (LW)-sensitive opsin mRNAs, respectively (Pohl et al. 2009). Moreover, the potential for variation in opsins among these butterflies was demonstrated in a separate study where the λ_{max} values of the LW-sensitive rhodopsins were shown to differ by as much as 31 nm (Frentiu et al. 2007a). In this study, we investigate the visual photopigments of *Adelpha fessonia* using next-generation sequencing. We first extracted RNA from eye and brain tissue of *A. fessonia* and related species and built transcriptome assemblies. We then quantified opsin expression levels using this RNA-seq data. We used epi-microspectrophotometry (epi-MSP) and optophysiology to measure the λ_{max} values of *A.*

fessonia LW- and UV-sensitive photopigments, respectively. We inferred the λ_{max} value of the *A. fessonia* blue-sensitive photopigment using comparative sequence analysis and functional expression data for *Adelpha/Limenitis* blue absorbing rhodopsins. We then modeled *A. fessonia* color vision using the spectral sensitivities generated from this study. Color space modeling of model and mimic wing coloration provides evidence that the orange patches of *Adelpha* wings may be a predator-specific signal whilst *A. fessonia* may be able to use achromatic vision to distinguish conspecifics from co-mimics by the differential brightness of the white stripes of their wings. Our efforts represent the first comprehensive study of the visual system of a butterfly species in the genus *Adelpha* and lays the foundation for future studies of the contribution of *Adelpha* butterflies' vision to the evolution of anti-predator defenses including mimicry.

Materials and Methods

Photographs of butterflies

Whole mount specimen photos were taken with a Canon 5D Mk III and Canon 100mm f/2.8L macro lens with an off camera diffused flash. Each head photo is a stack of 50 photos taken with a Canon 5D Mk III and Canon MP-E 65mm 1-5x macro lens under constant, diffused lighting. Plane of focus was incrementally moved from the front to the back of the head with an automated slider rail. Photos were stacked with Zerene Stacker v.1.04 (Zerene Systems LLC, Richland). Final composite photos as well as

whole mount photos were edited with Adobe Photoshop Lightroom 6 to adjust exposure and color correction.

Photographs of butterfly eyeshine

The apparatus for eyeshine photos was the same as for epi-microspectrophotometry (for details, see Fig. 1 of Briscoe and Bernard 2005). Briefly, it is a Leitz Ortholux-Pol microscope equipped with a Leitz 620-257 low stray-light Epi-illuminator, fed by a 45 w quartz-halogen lamp in an Ealing housing. Optics were a Leitz 8X/0.18P objective and 16X eyepieces. A Uniblitz shutter controlled exposure time. An Olympus TG-1 digital camera was attached to an eyepiece. Settings of the camera were: macro; iso 1600; zoom 4.0; focal length 18; metering mode 3; F/4.9; exposure program 2; color profile sRGB IEC61966-2.1; and 1920 x 2560 pixels. An intact butterfly was mounted in a slotted plastic tube fixed to the goniometric stage, then oriented to set the eye's direction of view. The microscope was adjusted to center the eyeshine patch in the field of view, focused on the cornea. After several minutes of dark-adaptation, a photo was taken using a 0.5 sec flash.

Specimen collection, RNA extraction, Sanger sequencing and RNA-seq

Ebel et al. (2015) demonstrated that Eurasian and North American *Limenitis* species are embedded in North American *Adelpha* making the genus *Adelpha* paraphyletic. We follow Willmott (2003a) and the more recent updates by Prudic et al. (2008) and Rush et

al. (2023) for *Adelpha* taxonomy. Adult butterflies from eight *Adelpha* species (*A. basiloides, A. californica, A. celerio, A. donyssa, A. ethelda, A. iphiclus, A. leucerioides, A. pithys*) and three *Limenitis* species (*L. lorquini, L. weidemeyerii,* and *L. archippus*) were initially collected from various localities in Oaxaca, Mexico and the U.S.A. in 2007-2009 and used for Sanger sequencing. Adult individuals from ten additional species (*A. boreas, A. cocala, A. cytherea, A. erotia, A. heraclea, A. leucophthalma, A. malea, A. naxia, A. phylaca* and *A. celerio*) were subsequently collected from Costa Rica in 2015-2017 using aerial insect nets, or were reared on host plants on which they were found in the field [permit #'s: R-003-2016-OT-CONAGEBIO; R-021-2016-OT-CONAGEBIO]. *Limenitis arthemis astyanax* was collected in Florida in 2016 and *A. fessonia* was obtained from the Costa Rica Entomological Supply in 2017 and these specimens were used for RNA-seq. Live adults were dissected into RNAlater (Invitrogen) by removing and bisecting the head between the eyes, removing the walking legs, and cutting the thorax in half between the middle and hind legs and removing the abdomen then submerging the tissues in RNAlater solution. Tissues were stored in a refrigerator whenever possible in the field and stored at -20° C upon arriving at the laboratory. Specimen collection locality data is given in Table 1.

RNA was extracted from all specimens using the Trizol (Invitrogen) extraction method. Opsin sequences for *A. iphiclus, A. leuceroides, A. basioloides, A. ethelda, A. donyssa, A. pithys, L. weidemeyerii, L. lorquini, L. archippus,* and *A. californica* were obtained using RT-PCR with degenerate PCR primers and direct Sanger sequencing of the PCR products (see Frentiu et al. 2007b for methods). For the other samples, TruSeq RNA

Sample Preparation Kit v2 (Illumina) was used to prepare libraries for 100 bp paired-end RNA-seq. Sequencing was done on a HiSeq 2500 at the UCI Genomics High-Throughput Facility.

De novo transcriptome assembly

We built head tissue *de novo* Trinity assemblies for each of 11 *Adelpha* and 1 *Limenitis* species (Table 2). Raw reads were trimmed for quality and parsed using custom scripts. To create the *de novo* transcriptome assemblies, we used the Trinity pipeline (trinityrnaseq_r2012-06-08v2) on the University of California's Legacy High Performance Computing cluster (HPC2) (Grabherr et al. 2011; Haas et al. 2013). We deposited the resulting Trinity assemblies for *A. boreas, A. celerio, A. cocala, A. cytherea, A. erotia, A. fessonia, A. heraclea, A. leucophthalma, A. malea, A. naxia, A. phylaca* and *Limenitis arthemis* in Dryad (DOI: XX.XXXX/XXXXXX) and the corresponding raw RNA-seq data in ArrayExpress under E-MTAB-XXX.

The transcriptomes were searched for opsin sequences using BLASTX and *Heliconius melpomene* opsin query sequences (Macias-Munoz et al. 2019). Sequences with identity of more than 20% and an e-value greater than 1E-10 were extracted and translated into amino acid sequence using Orf Predictor with the blastx option before testing their homology by reciprocal blast hit (Min et al. 2005). UV, B and LW opsin sequences from *Adelpha* and *Limenitis* species either obtained through Sanger or RNA sequencing were annotated and deposited in GenBank with accession numbers: XXXXXXX-XXXXXXX (Table 1).

Phylogenetic Analysis

The evolutionary history of each opsin gene family member was inferred by translating and then aligning the complete nucleotide coding sequence for each opsin. After manual inspection, the maximum likelihood method based on the Tamura-Nei model (Tamura and Nei 1993) as implemented in MEGA7 (Kumar et al. 2016) was used to build trees rooted with outgroup nymphalid taxa, *Danaus plexippus* and *Vanessa cardui*. Initial tree(s) for the heuristic search were obtained by applying Neighbor-Join and BioNJ algorithms to a matrix of pairwise distances estimated using the Maximum Composite Likelihood (MCL) approach, and then selecting the topology with the highest log likelihood value. Support for each node was evaluated out of 100 bootstrap replicates.

Quantifying opsin gene expression in *Adelpha fessonia*

To determine the involvement of opsins in vision, we looked at the mRNA expression levels of the three *A. fessonia* visual opsins (ultraviolet, blue and longwave) along with four other members of the opsin gene family (unclassified opsin, RGR-like opsin, pteropsin, and RH7)(Macias-Muñoz et al. 2019) in eye + brain tissue using Kallisto (v0.46.2) RNA quantification (Bray et al. 2016). A custom BLAST database was made from the *de novo* Trinity assembly for *A. fessonia*. Protein query sequences for each opsin gene of interest were aligned against the custom BLAST database and corrected *A. fessonia* sequences were added to the *de novo* transcriptome assembly.

Transcriptome-wide gene expression (in TPMs) was then quantified in Kallisto by matching reads from *A. fessonia* RNA-seq libraries to k-mer type in pseudoalignments as opposed to direct read alignments (Bray et al. 2016). Expression levels were visualized by graphing the log base 2 of the TPM for each gene.

Testing for selection in the blue opsins of *Adelpha*

Adelpha blue opsins have either a tyrosine or a phenylalanine at amino acid position 195. This amino acid substitution causes a spectral tuning shift in *Pieris rapae* and *Limenitis arthemis* blue-absorbing rhodopsins (Frentiu et al. 2015; Wakakuwa et al. 2010). The Y195F substitution red shifts the blue opsin's peak from ~431 nm to ~435 nm. To identify possible positively selected sites, we first generated opsin sequence alignments in MEGA-X (Kumar et al. 2016; Yang and Nielsen 2002). Then we used a site-specific maximum likelihood model to test for selection. We made the assumption that the ratio of nonsynonymous to synonymous substitution rates (ω) is constant across the branches of the phylogeny but possibly different among sites. The multiple sequence alignments and phylogenetic trees were analyzed in EasyCodeML, a graphical frontend for PAML 4.9j (Phylogenetic Analysis by Maximum Likelihood) (Gao et al. 2019; Yang 2007). Site models used were M1a vs M2a (neutral vs positive) where support for positive selection is given if M2a provides a better fit than M1a using likelihood-ratio tests (Edgar 2004; Kumar et al. 2018; Yang et al. 2000).

Epi-microspectrophotometry

In vivo reflectance spectra of nymphalid butterfly eyeshine can be used to determine the absorbance spectrum of a long wavelength-absorbing visual pigment (LW rhodopsin) due to the rapid decay of the metarhodopsin photoproduct and relatively slow recovery of rhodopsin (for details see Frentiu et al. 2007b Supplementary materials). Repeated flashes of bright long-wavelength light convert a substantial fraction of LW rhodopsin to metarhodopsin, which then decays exponentially leaving the eye in a partially bleached state. With sufficient additional time in the dark there is substantial recovery of rhodopsin, so that difference spectra compared to the partially bleached state is an estimate of the absorbance spectrum of LW rhodopsin.

Spectral measurements of eyeshine from *Adelpha* spp. are challenging because their corneas exhibit structural, iridescent reflections that are a source of substantial glare, perturbing measurements from the fully dark-adapted eye. To reduce the influence of corneal glare from *A. fessonia*, the eye was treated for ten hours with 1 sec 566 nm flashes every 90 sec, which created a total bleach of LW rhodopsin and very bright eyeshine. Allowing rhodopsin to recover in the dark for two hours created a difference spectrum that was fit very well by a R530 rhodopsin template.

A similar strategy was employed for *A. californica*. A bright partial bleach was created with forty minutes of 5 sec Schott OG590 flashes every 60 sec. A reference spectrum was measured after waiting for metarhodopsin to decay. Then the eye was treated with a single 3 sec Hoya O58 flash, and a second spectrum measured after metarhodopsin decayed. The difference spectrum was well fit by the R530 template.

Optophysiology

Photoreceptor cells of butterfly eyes exhibit intracellular pupillary responses to bright light that cause easily measured decreases in eyeshine reflectance. Spectral sensitivity functions can be measured in a double-beam epi-MSP. The monitoring beam is set up to measure continuously the reflectance of eyeshine from the deep pseudopupil, with long-wavelength light that itself is so far below threshold that there is no decrease in reflectance after that beam is first turned on. The stimulating beam, from a wavelength-adjustable and intensity-adjustable monochromatic source, presents flashes to the eye that are sufficiently bright to cause decreased monitoring reflectance. To eliminate stimulus artifacts in these measurements, the quantum-counting photomultiplier is covered by a cutoff filter that transmits the monitoring beam but blocks the stimulating flashes.

It is important to choose the wavelength content of the monitoring beam, so it is reflected well by the tapetum. For most nymphalids, the tapetum reflects well from the UV out to a long-wavelength cutoff ranging from 650 nm to 700 nm or more, depending on the species and the eye-region. For *A. fessonia* and *A. californica*, however, the cutoff wavelength is only 600 nm, beyond which the reflectance drops abruptly. For our experiment with an *A. fessonia* female, therefore, we chose a monitoring beam created by a 600 nm interference filter covered by a density 2.0 neutral filter. The eye region selected was the same as for the epi-MSP bleaching experiment. The stimulus-blocking filter covering the PMT was Schott OG590. Stimulating flashes of either 60 sec or 10 sec duration were delivered every 4 min, as required to achieve stable response by the

end of the flash. The criterion response chosen was a 7% decrease in reflectance monitored and recorded by a digital oscilloscope. For wavelengths ranging from 340 nm to 580 nm every 10 nm, the criterion response was achieved. At the end of the experimental session, all quantum fluxes that created criterion responses were measured with a factory-calibrated Hamamatsu S1226BK photodiode. The spectral sensitivity data were computed as the reciprocal of those quantum fluxes vs wavelength. The good fit of an R355 template to the pupillary sensitivity data shows that only the UV-sensitive R355 photoreceptors contribute to responses in the range 340 nm – 380 nm. Similarly, the fit of an R530 template from 490 nm – 580 nm shows that only the green-sensitive R530 receptors contribute to long-wavelength sensitivity, confirming the MSP estimate that the L rhodopsin of *A. fessonia* is R530. In the range 390 nm – 480 nm, the elevated sensitivity of data argues for a contribution from blue-sensitive rhodopsin, but its spectral position was not determined in these experiments.

HEK293 cell culture expression, reconstitution, and UV-visible spectroscopy of BRh visual pigment

In a previous site-directed mutagenesis study of *Adelpha/Limenitis* BRh opsins, we identified a Y195F substitution which led to a ~4 nm spectral red shift in peak absorbance of the reconstituted photopigment relative to the wildtype BRh opsin that had a Y at site 195 (Frentiu et al. 2015). In that study, however, we did not report data from a wild-type BRh opsin sequence with F at site 195. Since *A. fessonia* and *A. basiloides* differ at this site, we decided to report below the outcome of expressing a wildtype BRh opsin which is very similar in sequence and which has a F amino acid at

site 195, namely that of *L. lorquini*. Methods for the functional expression of *L. lorquini* are detailed in Frentiu et al. (2015). Total RNAs were extracted from a single adult *L. lorquini* head using Trizol (Invitrogen). cDNAs were then synthesized using a Marathon cDNA amplification kit (BD Biosciences, Franklin Lakes, NJ). The BRh coding region was cloned into pGEM-T easy vector (Promega). A short oligonucleotide sequence encoding the 1D4 epitope of bovine rhodopsin (STTVSKTETSQVAPA) was added before the stop codon. The tagged cDNA fragments were subcloned into expression vector pcDNA3.1(+) (Invitrogen). Transient transfection of HEK293 cells by plasmid DNA was carried out by Lipofectamine 2000 (Invitrogen). The cells were replated 2 days after transfection and treated with 1 mg/mL G418 sulfate (EMD Chemicals Inc., Gibbstown, NJ) for 2 weeks. Twelve cell clones were chosen, expanded, and screened by western blotting. The clone having the highest expression level was then expanded to 15 plates of cells. The cultured cells were incubated with 1 mM 11-*cis*-retinal for 2 days and collected by centrifugation under dim red light. The collected cells were incubated with 40 mM 11-*cis*-retinal for 1 h at 4 °C. The reconstituted visual pigments were extracted using 1% n-dodecyl b–D-maltoside (DDM) (Sigma-Aldrich, Saint Louis, MO) in 10 ml of extraction buffer (pH 6.7) (250 mM sucrose, 120 mM KCl, 10 mM MOPS, 5 mM MgCl2, 1 mM DTT, 1 Roche protease inhibitor cocktail tablet) (Vought et al. 2000) via gentle rotation for 1 h at 4 °C. The visual pigments were then purified by immunoaffinity chromatography. Briefly, the crude extract was mixed with Sepharose beads conjugated with 1D4 IgG (University of British Columbia, Canada) overnight at 4 °C. The beads were then washed with 50 ml of wash buffer, pH 6.6 (20% glycerol, 120mM KCl, 5mM MgCl2, 50mM HEPES, and 0.1% DDM) (Vought et al. 2000). The

visual pigments were eluted with 50 mM competing peptide (Quality Controlled Biochemicals, Hopkinton, MA) in wash buffer and measured in a Hitachi U-3310 UV-Vis spectrophotometer at 0°C. Spectral data represent the average of 5–8 scans. λ_{max} was estimated by least-squares fitting of the data to a visual pigment template (Stavenga et al. 1993).

Reflectance of *Adelpha fessonia* and *A. basiloides* wings

Wings of *A. fessonia* samples were obtained from live specimens purchased from the Costa Rica Entomological Supply while *A. basiloides* wings were obtained from dry specimens in the collection of the Museo de Zoología Alfonso L. Herrera in the Universidad Nacional Autónoma de México. Dry samples were rehydrated overnight before wings were excised. Wing reflectance measurements of 3 males and 2 females each of *A. fessonia* and *A. basiloides* (n=10 butterflies total) were taken using previously described methods (Bybee et al. 2012; Finkbeiner et al. 2017b).

Briefly, measurements were taken on the orange spots and white stripes of their right forewings as these patches could possibly elicit responses from conspecifics or avian predators. The fixed probe holder (Ocean Optics RPH-1) was placed so that the axis of the illuminating and detecting bifurcating fiber (Ocean Optics 400-7-UV/VIS) was 45 degrees to the plane of the wings. Illumination was provided by a deuterium-halogen tungsten lamp (Ocean Optics DH-2000) with the reflectance spectra measured by an Ocean Optics USB2000 spectrometer. Measurements were recorded on OOIBase32 and smoothed and plotted using the r package, “pavo” (Maia et al. 2019).

Visual modeling of *Adelpha fessonia* wings through the eyes of predator and prey

We used the receptor-noise model to predict whether *A. fessonia* and avian predators can distinguish between *A. fessonia* and *A. basiloides* orange patches and white stripes (Vorobyev and Osorio 1998). The reflective distribution of the measured stimuli from the reflectance measurements were plotted on a triangular *A. fessonia* color space and avian tetrahedral color spaces of ultraviolet and violet capable birds. Using the "vismodel" function from "pavo", we calculate the quantum catches at each photoreceptor. For the avian models, we use the built-in averages for UV-sensitive and violet-sensitive visual systems for chromatic distances and the double-cone sensitivity of the blue tit and chicken for luminance distances of UV-sensitive and violet-sensitive, respectively. For *A. fessonia*, we use λ_{max} values corresponding to 355 nm, 431 nm, and 530 nm, respectively, for the chromatic distances and the 530 nm photoreceptor for luminance distances. The color spaces were then generated using the "plot" and "colspace" functions (Maia et al. 2019).

Chromatic and achromatic distances between the orange patches and white stripes in *A. fessonia* and *A. basiloides* were calculated using the "bootcoldist" function. Bootcoldist allows us to perform a bootstrap measurement with a 95% confidence interval to determine if the color distance measurement exceeds a theoretical discrimination threshold (Maia et al. 2019). A JND threshold of one is typically used. However, spectra separated by a JND threshold of one could still be impossible to distinguish between each other and so we use a threshold of two as used for bird

plumages (Meneses-Giorgi and Cadena 2021). We use a relative receptor density of 1:2:2:4 (ultraviolet:short:medium:long-wave receptors) along with a Weber fraction of 0.1 for both chromatic and achromatic receptors for the UV-sensitive bird model (Kelber et al. 2003; Maier and Bowmaker 1993). For the violet-sensitive bird model, we use a relative receptor density of 1:2:4:4 (short:short:medium:long) as well as a Weber fraction of 0.1 for both chromatic and achromatic receptors (Kram et al. 2010). Over a period of years we tried to obtain additional pupae of *A. fessonia* from our Costa Rican source to perform *in situ* hybridization on this species but were unsuccessful. Therefore, *Adelpha fessonia*'s relative receptor density of 0.15, 0.13, 1 (UV:short:long) was approximated from a *Limenitis arthemis* opsin *in situ* hybridization image (Frentiu et al. 2015). Photoreceptor density was manually performed by counting a random sample of 102 intact ommatidia and normalizing the photoreceptors in proportion to the long-wave sensitive photoreceptor. We used a Weber fraction of 0.05 for both chromatic and achromatic receptors (Koshitaka et al. 2008). Illumination and background settings were set to forest shade and green, respectively, to simulate the natural habitat of *Adelpha* butterflies and their avian predators. Calculated color distances were then plotted using rstudio's "plot" function.

Results

Adelpha fessonia has sexually monomorphic eyes

Photographs of *A. fessonia* compound eyes and eyeshine do not show any obvious dimorphism between the two sexes (Fig. 1C-F). Eyes of both sexes are characterized

by heterogeneity in the color of the eyeshine across the retina with blue, green, and yellow-green-reflecting ommatidia (Fig. 1E, F). The lack of red ommatidia suggests an absence of red-sensitive photoreceptor cells (with $\lambda_{max} \geq$600+ nm) in *A. fessonia*. A previous study found that in the ommatidia of nymphalids without saturated red eyeshine, there was no evidence for R3-8 photoreceptor cells that were red-sensitive (Briscoe and Bernard 2005). This does not preclude, however, a second class of long wavelength-sensitive photoreceptor cell with a peak sensitivity >530 nm due to optical filtering of the basal R9 cell by the overlying R1-8 photoreceptor cells (Belušic et al. 2021). Even without evidence for red-sensitive photoreceptor cells, it is still expected that *A. fessonia* will have UV-, blue- and LW-sensitive photoreceptor cells, corresponding to each kind of opsin.

UV, blue and LW visual opsins of *Adelpha fessonia*

Indeed, our BLAST searches of the *A. fessonia* transcriptome assembly yielded three visual opsin transcripts corresponding to one UV, one blue, and one LW opsin and three additional transcripts encoding an RGR-like opsin, a pteropsin, and Rh7 opsin. A similar number of visual opsin transcripts (n=3) was found in the other surveyed *Adelpha/Limenitis* species except for *A. leucerioides,* where we found two LW opsin mRNA transcripts, and evidence of a species-specific gene duplication (Fig. 2C). Across all three visual opsin phylogenies constructed using the expanded RNA-seq data, the following sister taxa were recovered: *A. heraclea* - *A. naxia, A. boreas* - *A. leucerioides, A. donyssa* - *A. pithys,* and *A. celerio* - *A. californica,* although the bootstrap support for

A. boreas - *A. leucerioides* was <60% (Fig. 2A-C). The genus *Limenitis* was recovered as a monophyletic clade with high bootstrap support. Lastly, the site-specific maximum likelihood model showed no evidence of positive selection occurring among the blue opsin gene in *Adelpha* lineages.

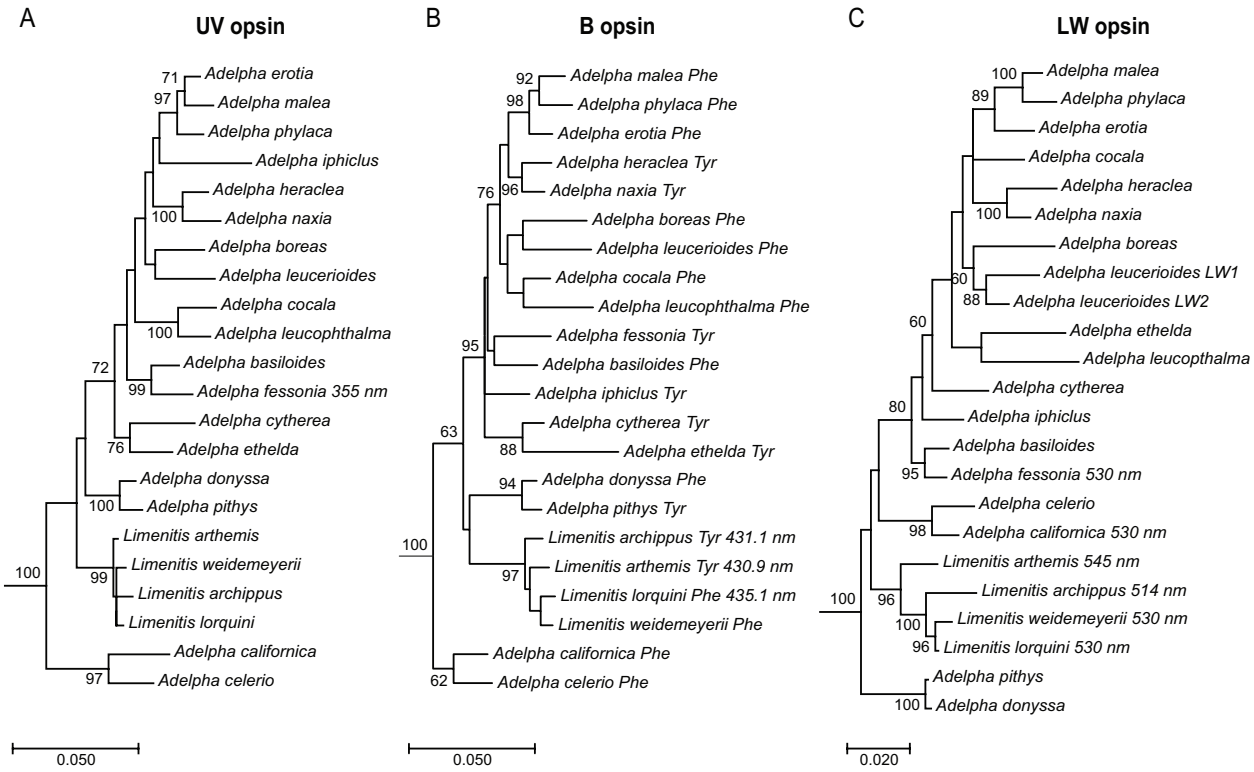

Figure 2. Phylogenies of *Adelpha* UV, blue, and LW opsins. (A) UV, (B) blue and (C) LW opsin nucleotide phylogenies reconstructed using maximum likelihood, the Tamura-Nei model (Tamura and Nei 1983), and 100 bootstrap replicates. Bootstrap support values <60% are not shown. The blue opsin amino acid at site 195, either phenylalanine (Phe) or tyrosine (Tyr), is shown for each species together with λ_{max} values of the blue-absorbing *Limenitis* rhodopsins (Frentiu et al. 2015). λ_{max} values of the LW-absorbing

rhodopsins are also shown (Frentiu et al. 2015). Scale bar = substitutions/site. A recent duplication of the LW opsin gene is observed in *A. leucerioides*.

Visual opsins mRNAs are highly expressed in *A. fessonia* heads

We found that the UV, blue, LW, and unclassified opsins were highly expressed in *A. fessonia* head tissue while RGR-like opsin, pteropsin, and RH7 were not (Fig. 3). The LW opsin was the most highly expressed whereas the blue and UV opsin followed closely with similar expression levels. This is to be expected as these three opsins are expressed in the compound eyes of *Limenitis* (Frentiu et al. 2015). The unclassified opsin, a candidate retinochrome, was also highly expressed though not as high in comparison to another nymphalid butterfly, *Heliconius melpomene* (Macias-Muñoz et al. 2019). In addition, the expression levels of the RGR-like opsin are much lower than that of *H. melpomene*. However, this may be due to differences in the times of day that the tissue were harvested and/or in the size of photoreceptor cells relative to secondary pigment cells within which the visual opsins and unclassified opsin, respectively, are expressed.

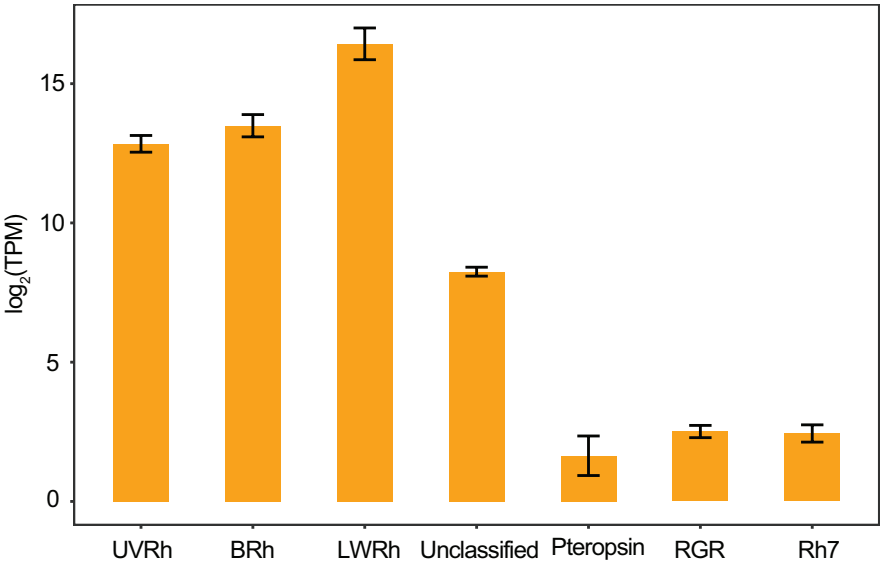

Figure 3. Expression of opsin genes in *Adelpha fessonia* eye + brain tissue (n=5) measured using RNA-seq data and Kallisto quantification. Y-axis is in transcripts per million on a $\log_2$ scale. Error bars indicate standard error.

λ_{max} values of *Adelpha fessonia* LW and UV rhodopsins

Adelpha fessonia and *A. californica* LW rhodopsins from dark adapted and partially bleached eyes show peak absorbance at 530 nm (Fig. 4A) similar to the λ_{max} values of *Limenitis lorquini* and *L. weidmeyerii* (Frentiu et al. 2007a,b; Frentiu et al. 2015.

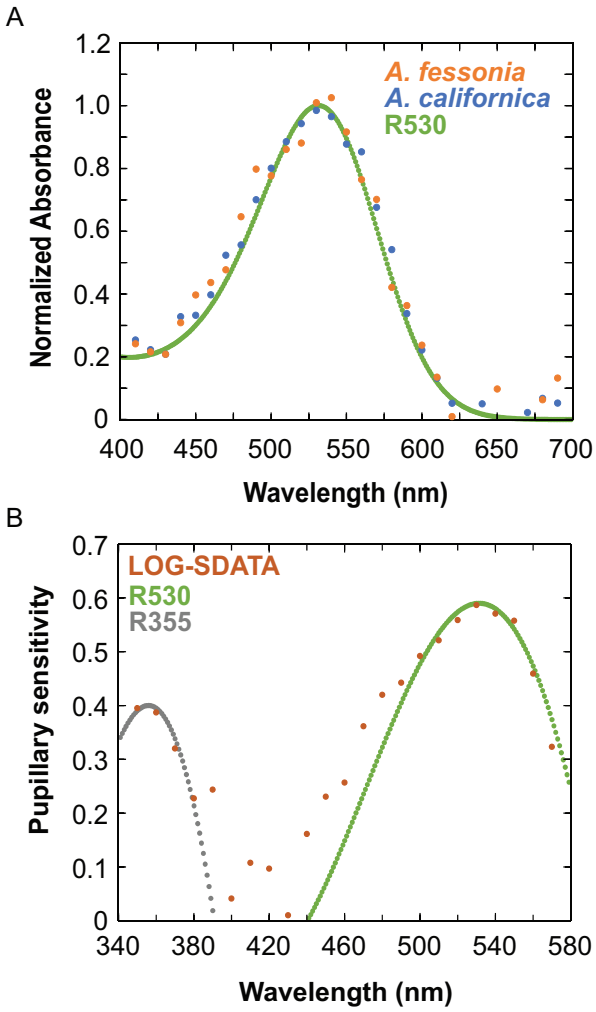

Figure 4. Epi-microspectrophotometry and pupillary sensitivity of *Adelpha fessonia* eyes. (A) Normalized absorbance spectra of *Adelpha fessonia* and *A. californica* long wavelength-absorbing rhodopsins. Dots indicate experimental spectra of *A. fessonia* (orange) and *A. californica* (blue) and green dotted lines indicate rhodopsin template with peak absorbance at 530 nm (R530) (Palacios et al. 1996). (B) *A. fessonia* UV- and long wavelength rhodopsin sensitivity measured using optophysiology. Experimental pupillary sensitivity of *A. fessonia* (orange dots). Dotted lines indicate fits to a computational model which includes both R355 (grey) and R530 (green) rhodopsins.

Pupillary sensitivities of *A. fessonia* peak in the UV and LW

The pupillary sensitivity data of *A. fessonia* as shown in Fig. 2B was computed as the reciprocal of quantum fluxes versus wavelength. The good fit of an R355 template to the pupillary sensitivity data shows that only the UV-sensitive R355 photoreceptors contribute to responses in the range 340-380 nm. Similarly, the fit of an R530 template from 490-580 nm shows that only the green-sensitive R530 receptors contribute to long-wavelength sensitivity, confirming the epi-microspectrophotometry estimate that the LW rhodopsin of *A. fessonia* is R530. In the range 390-480 nm the elevated sensitivity of data argues for a minor contribution from a blue-sensitive rhodopsin, but its spectral peak could not be determined from these experiments. Pigments in the 530 nm region are the most abundant and easiest pigments to measure, hence the higher sensitivity when compared to the peaks near R355. The experimentally determined 355 nm and 530 nm peaks of *A. fessonia* physiological response to light are driven by the UV- and LW-sensitive photopigments. The differing abundances of each pigment and the photoconversions of each rhodopsin to metarhodopsin (which has a peak in the bluish range) make it difficult to measure the λ_{max} value of the blue-absorbing rhodopsin.

The blue-absorbing rhodopsins of *Adelpha/Limenitis*

To bypass technical challenges of measuring the blue rhodopsin *in vivo* using either epi-microspectrophotometry or optophysiology, we aligned and compared the blue opsins of

22 species in the *Limenitis/Adelpha* genera. Then we used absorbance spectra data from HEK293-expressed rhodopsins of species in the *Limenitis* clade to infer the absorbance peaks of the *Adelpha fessonia* blue-sensitive rhodopsin, including data from a previously unstudied species and close relative of *A. fessonia*, *L. lorquini*.

The blue-absorbing rhodopsin of *Limenitis lorquini* has a peak absorbance at 435.1 nm and a phenylalanine at the known spectral tuning site, amino acid 195 (Fig. 5A, D). *Limenitis arthemis* and *L. archippus* have peak absorbances of 430.9 nm and 431.1 nm, respectively (Frentiu et al. 2015), and both have a tyrosine at amino acid 195 (Fig. 5B and C). A substitution of phenylalanine to tyrosine at amino acid 195 in *L. arthemis* results in a red-shifted pigment with a λ_{max} of 435.1 nm (Fig. 5C). As seen from the amino acid alignment in Fig. 5D, *A. fessonia* has tyrosine at position 195 suggesting that the blue-absorbing rhodopsin of *A. fessonia* has a peak absorbance at around 431 nm.

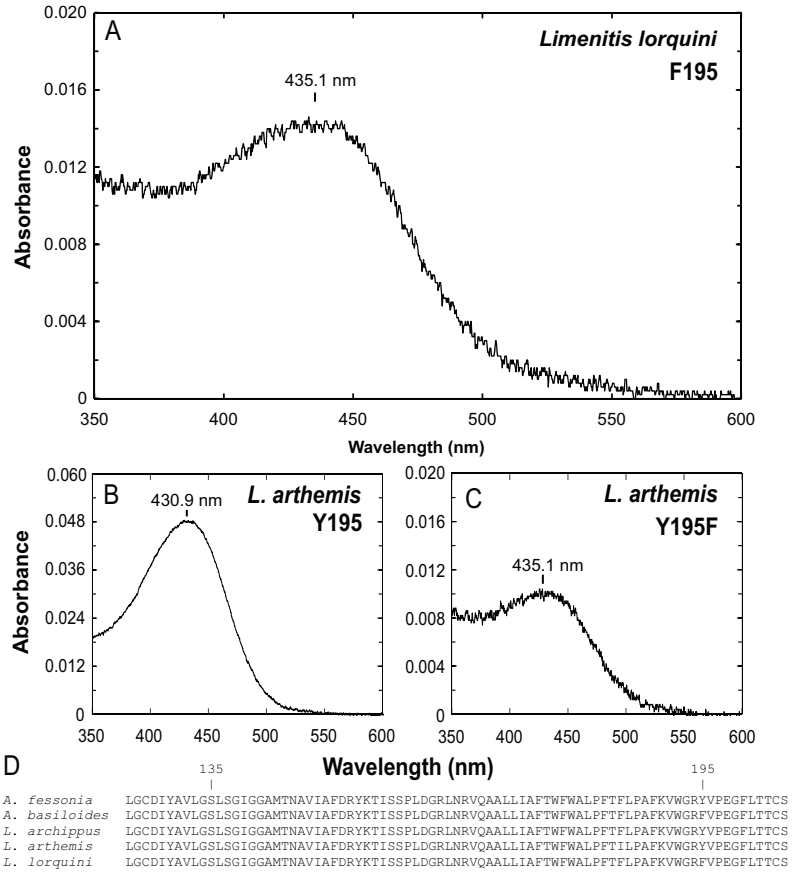

Figure 5. *Limenitis* blue-absorbing rhodopsin dark spectra based on heterologous expression in HEK 293 cells. Dark spectra of (A) wildtype *Limenitis lorquini*, (B) wildtype *L. arthemis* and (C) F195Y mutant *L. arthemis* blue-absorbing rhodopsins. Spectra of (B) and (C) reproduced with permission from Frentiu et al. (2015). (D) Partial amino acid alignment of the blue opsin of representative species indicating the location of two amino acid sites, 135 and 195, with known spectral tuning effects (Wakakuwa et al. 2004; Frentiu et al. 2015; Liénard et al. 2021).

Adelpha fessonia may distinguish white wing stripes that avian predators probably cannot

The dorsal white stripes and orange patches of most *Adelpha* wings look mostly indistinguishable between species (Fig. 6A) and so we investigated if this is also true for *A. fessonia* and their avian predators. The white stripes on the dorsal portion of *A. basiloides* show brighter reflectance in the 300 to 500 nm range compared to *A. fessonia* wings while the orange patches overlapped throughout the UV-vis range (Fig. 6B).

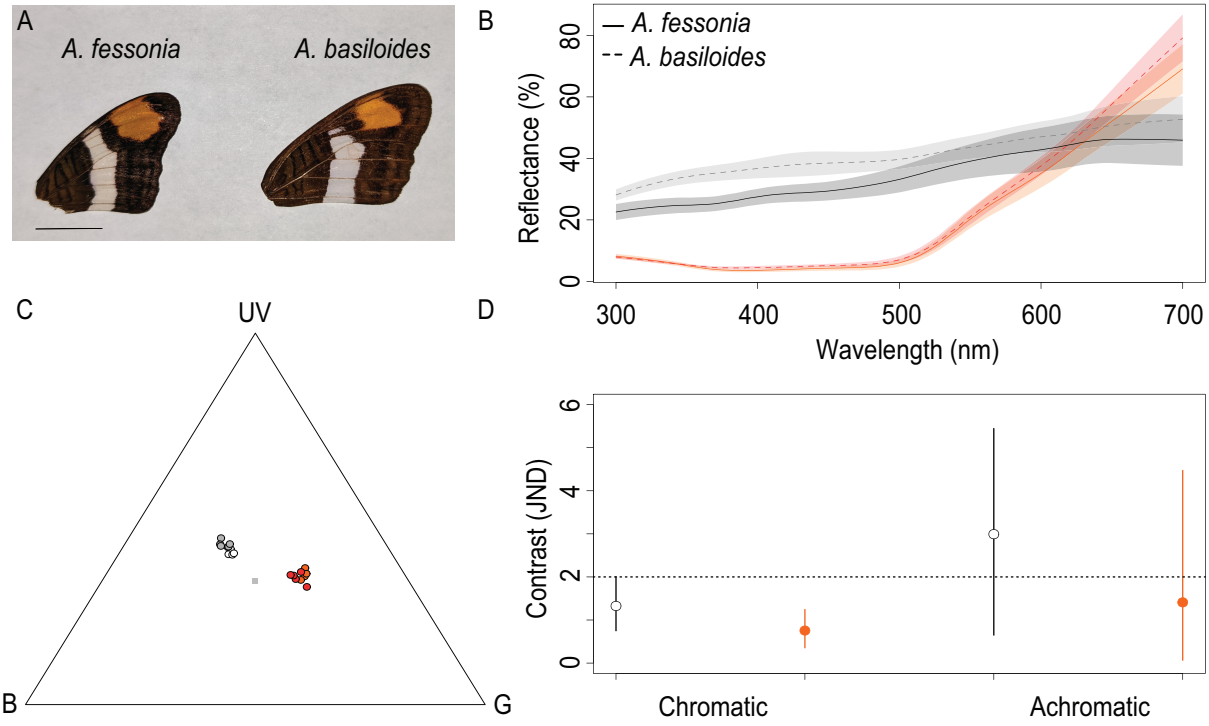

Figure 6. Visual modeling suggests *Adelpha fessonia* and *A. basiloides* white wing patches are distinguishable achromatically when viewed through the eyes of *A. fessonia*. (A) Photographs of dorsal right forewings of *A. fessonia* (left) and *A. basiloides*

(right) with scale bar representing 1 centimeter. (B) Reflectance measurements of *A. fessonia* orange wing patch (orange), *A. fessonia* white wing stripe (black), *A. basiloides* orange wing patch (dashed red), and *A. basiloides* white wing stripe (dashed grey). (C) *A. fessonia* orange patch (orange), *A fessonia* white stripe (white), *A. basiloides* orange patch (red), and *A. basiloides* white stripe (grey) mapped in the trichromatic color space for the *A. fessonia* visual system. (D) Distances between the two species' wing color patches as viewed through the *A. fessonia* visual system. Color distances are in units of chromatic contrast (JND) between *A. fessonia* and *A. basiloides* wings with a JND threshold (dotted line) of 2. Points and bars are bootstrapped mean values with 95% confidence intervals.

Chromatic diagrams show that the clusters for the orange patches and white stripes overlapped in both *A. fessonia* and the two bird (UV and violet) visual models (Fig. 6C, 7A and C). All three models did not pass the JND threshold of two in the chromatic space for the orange patches or the white stripes. This is also the case when looking at achromatic calculations for the orange patches (Fig. 6D, 7B and D). However, *A. fessonia* did exceed the JND threshold for the white stripes in the achromatic contrast space (Fig. 6D) while both violet- and UV-sensitive bird systems did not (Fig. 7B and D). As predictive tools, these models will require behavioral studies to confirm.

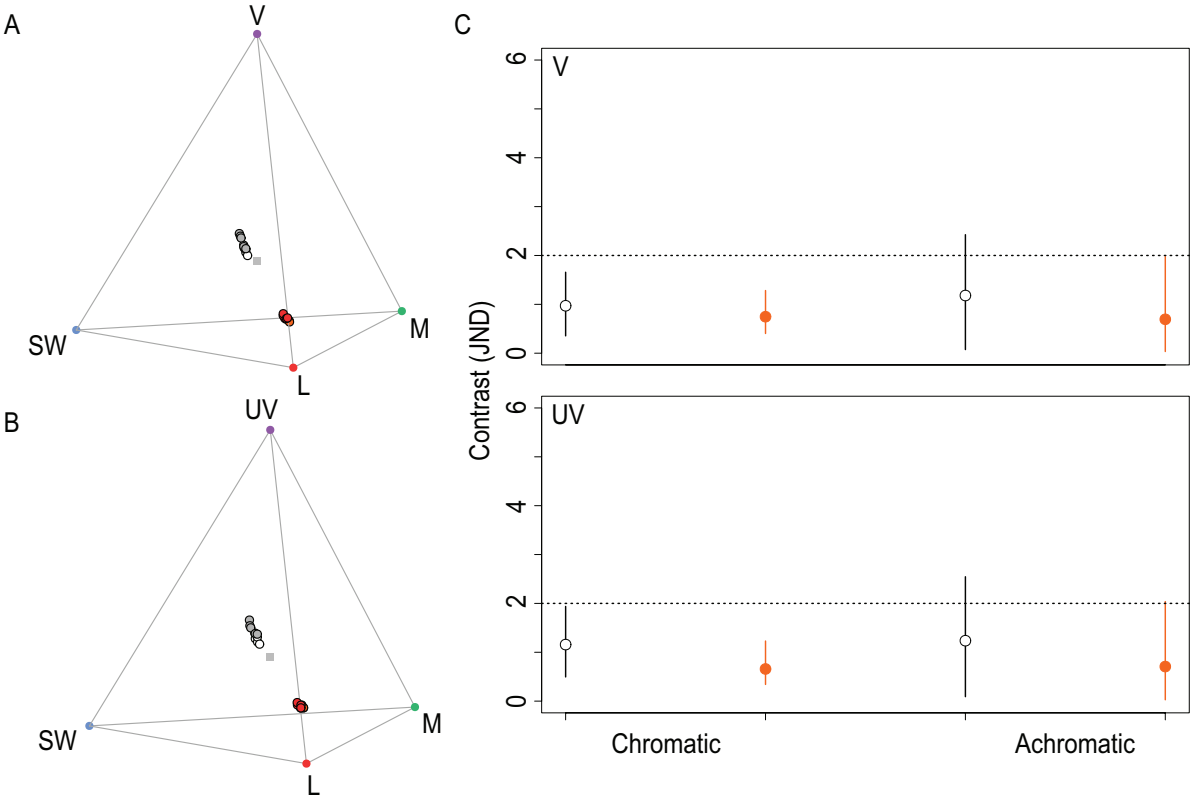

Figure 7. *Adelpha fessonia* and *A. basiloides* orange patches and white stripes are likely indistinguishable to avian predators. Coloration of *A. fessonia* orange patch (orange), *A fessonia* white stripe (white), *A. basiloides* orange patch (red), and *A. basiloides* white stripe (grey) in tetrahedral color spaces for violet-sensitive (A) and UV-sensitive (B) avian visual systems. (C) Color distances between *A. fessonia* and *A. basiloides* wing patches for violet-sensitive (top) and UV-sensitive (bottom) avian visual systems. Color distances are in units of chromatic contrast (JND) between *A. fessonia* and *A. basiloides* wings with a JND threshold (dotted line) of 2. Points and bars are bootstrapped mean values with 95% confidence intervals. UV=ultraviolet, V=violet, SW=blue, M=RH2, L=LWS.

Discussion

Our experiments allow us to characterize the photopigments of *Adelpha fessonia* eyes. As we have shown, *A. fessonia* possesses three photopigment types consistent with the potential trichromacy of other nymphalid butterflies. Our study has also shown that *A. fessonia* eyes are not obviously sexually dimorphic, measured the peak sensitivities of their photopigments, and quantified opsin gene expression levels. In addition, *A. fessonia* is unlikely to have color vision in the red range (>600 nm). Characterizing the photopigments of *A. fessonia* eyes allowed us to model *A. fessonia* vision and provide us with hints of their perception of the world. While these experiments were performed on *A. fessonia*, these findings are relevant to studying the evolution and ecology of visual perception in *Adelpha* butterflies more broadly.

The presence of heterogeneous eyeshine in butterfly eyes consisting of yellow- and red-reflecting ommatidia is not universal (Briscoe and Bernard 2005; Stavenga et al. 2001). While eyeshine could be locally uniform, there are instances where heterogeneity occurs that could be indicative of adaptations that optimize spectral discrimination in the yellow, orange and red range of the visible light spectrum. The patterns resulting from this heterogeneity can vary greatly between species though some species may share similar motifs. Lycaenidae, and certain nymphalid subfamilies, Nymphalinae and Charaxinae, share a red and yellow motif with the nymphalid subfamily Heliconiinae (Stavenga 2002). This red eyeshine in *Heliconius* butterflies is indicative of the presence of red photoreceptors resulting from the presence of filtering

pigments (Zaccardi et al. 2006) and of the presence of optical filtering by overlying photoreceptor cells (Belušic et al. 2021). These red filtering pigments have been demonstrated to cause behavioral differences in butterfly species that have them and those that do not. *Heliconius erato,* a species possessing red filtering pigments, was able to differentiate between red and orange stimuli while *Vanessa atalanta,* a species without red filtering pigments, was not (Zaccardi et al. 2006). *Adelpha fessonia* has a yellow/green/blue eyeshine pattern like what is seen in other nymphalids such as *Hypolimnas bolina,* denoting a lack of a red photoreceptor (Stavenga et al. 2001).

It was expected that *A. fessonia* vision would have three major spectral classes of photoreceptors as described in other nymphalids (Briscoe 2008). We expect genes involved in vision to be highly expressed in head tissue. RNA-seq quantification showed high expression levels of the three light sensitive opsin mRNAs (LW, blue, and UV) that are directly involved in vision along with an unclassified opsin that is also expressed in nymphalid butterfly secondary pigment cells (Fig. 3)(Macias-Muñoz et al. 2019). *Adelpha fessonia* has a low expression of RH7, a gene associated with light sensing circadian rhythms, unlike the high expression found in *Manduca sexta* (Feuda et al. 2016; Macias-Muñoz et al. 2019).

We found the peak absorbances (λ_{max}) of *A. fessonia* photopigments in the ultraviolet, blue, and long wavelength portions of the light spectrum corresponding to 355 nm, 431 nm, and 530 nm, respectively, based on optophysiology and epi-microspectrophotometry on living eyes as well on comparative sequence analysis (Figs. 4 and 5). Previously, amino acid substitutions at two sites were shown to be crucial for spectral tuning in blue-absorbing visual pigments in the small white butterfly, *Pieris*

rapae (Wakakuwa et al. 2010). In the case of *P. rapae*'s blue-absorbing pigment, a F to Y at position 177 caused a 4 nm blue shift. Conversely, site-directed mutagenesis of the opposite mutation (Y to F at site 195) in *Limenitis* BRh opsins caused the same magnitude of effect, although in the opposite direction (Fig. 3C-E and Frentiu et al. 2015). Importantly, functional expression of wildtype *L. lorquini* and mutant *L. arthemis astyanax* opsins, which both have a F at site 195 have the same peak absorbance of 435 nm, while wildtype *L. arthemis astyanax* and *L. archippus,* with a Y at site 195 both have a peak absorbance at 431 nm. Given the *A. fessonia* BRh shares a Y at site 195 with *L. arthemis* and *L. archippus*, it is highly likely its blue photopigment has a spectral peak at 431 nm, while that of *A. basiloides,* having a F at this site is likely to have a peak closer to 435 nm. Do these small spectral tuning effects have an impact on these butterflies' fitness? If so, then it is likely to be very small as we did not find any evidence of positive selection occurring in the blue opsins of the *Adelpha* lineage via a PAML site-specific test. The evolutionary reason behind why some species have the tyrosine phenotype and others have the phenylalanine phenotype is currently unknown but raises the question of whether or not this small tuning effect has an impact on the butterflies' visual capabilities. What are the evolutionary benefits of one phenotype versus another and why do some members of the *Adelpha*/*Limenitis* clade possess the tyrosine or the phenylalanine phenotype? How does their vision affect their vast diversity? Although differing peak sensitivities in *Adelpha* BRh photoreceptors could cause variation in their visual perceptions which might play a role in creating and maintaining the color of objects they interact with, available evidence suggest that BRh is evolving conservatively in *Adelpha/Limenitis* spp.

We have to make the distinction of whether or not phenotypic similarities are a byproduct of shared ancestry between sister species or of convergent evolution between two unrelated species. For example, *A. fessonia* and *A. basiloides'* similar wing patterns may be the result of shared ancestry as seen in their opsin phylogenies (Fig. 2). However, these phylogenies provide only weak evidence that *A. fessonia* and *A. basiloides* are sister species for several reasons. First, our species sampling in *Adelpha* is very incomplete relative to the diversity in the genus, with samples selected to span the diversity, rather than provide a test of species relationships. Furthermore, *A. fessonia* immature stages do not resemble those of *A. basiloides*, and *A. basiloides* is very likely sister to *A. plesaure* based on immature morphology and the phylogenetic analysis of Ebel et al. (2015). In addition, *A. fessonia* is thought to be sister to *A. gelania* based on similarities in their genitalia, despite looking different in wing pattern and wing shape (Willmott, 2003a). Supporting the hypothesis of convergent wing patterns is the fact that the putative sister taxa *Adelpha plesaure* and *A. gelania* do not resemble *A. basiloides* and *A. fessonia,* respectively. Whether or not their color patterns are the result of shared ancestry, it can be argued that these similar patterns are maintained because of mimicry as there would be little evolutionary incentive to diverge from an effective signal that advertises their unprofitability.

Butterflies are visually dependent creatures capable of discerning a plethora of visual stimuli (Finkbeiner et al. 2017b, Finkbeiner et al. 2021). Behaviors such as mate selection and host/food plant location have not been studied in-depth with *A. fessonia,* but with these data, the groundwork has been set to do so. Our study could also

potentially lead to better understanding of how mimetic nymphalids are able to correctly identify conspecifics for mating. *Adelpha fessonia* eye morphology and wing color patterns (in the visible spectrum) are not apparently sexually dimorphic (Fig. 1A-F). Due to their lack of a red sensitive opsin or a redshifting filtering pigment, *A. fessonia* is unlikely to possess red color vision. This means that they may not be able to distinguish the orange patches on the wings of their own versus another similar-looking species like *A. basiloides*. Even if their tiny R9 cell is red-shifted due to optical filtering by overlying photoreceptor cells, the orange wing reflectance spectra between the two species are likely to be too similar to be distinguishable to *A. fessonia*. Under either scenario, the orange aposematic signal is most likely used as a signal to ward off predators (Páez et al. 2021). As butterflies are capable of learning and distinguishing between small differences in wavelengths in visual stimuli, it is possible that *A. fessonia* is using other visual signal features to discriminate conspecifics from co-mimics (Koshitaka et al. 2008).

Our modeling provided evidence that *A. fessonia* can discriminate between the white stripes of *A. fessonia* and *A. basiloides* achromatically and that avian predators are unable to distinguish the two species' white stripes. Studies in color vision typically focus on the impact of chromatic cues and control for achromatic information (Kelber et al. 2003). However, most visual stimuli have a combination of chromatic and achromatic cues, and both should be accounted for when making predictions (Olsson et al. 2018). Recent studies have shown that achromatic cues do elicit behavioral responses, particularly in *Papilio xuthus* foraging behavior (Kinoshita et al. 2012). It is plausible that achromatic cues could be used in other ecological behaviors such as mate selection

and that *A. fessonia* is using the white stripe to determine conspecific individuals from *A. basiloides*. There is a vested interest for butterflies to distinguish conspecifics. Quickly finding conspecifics can improve mating success as the butterfly would not needlessly expend time or energy courting the wrong orange and white butterfly. In addition, hybridization between two different species typically results in a lower fitness for the hybrid such as the case of reduced feeding abilities in hybrid *Limenitis* butterflies (Kramer et al. 2018). In rare cases such as in *Heliconius* butterflies, speciation can occur via hybridization (Mavárez et al. 2006) though this is likely not an issue for *A. fessonia* and *A. basiloides*. Even though modeling is a powerful predictive tool, behavioral assays will still need to be done to confirm *A. fessonia* and bird color-discerning capabilities.

In this study, we have characterized the photopigments of *Adelpha fessonia* and modeled their visual capabilities. Using the measured peak sensitivities of their three photopigments, we created color space models to quantify their potential color discrimination abilities. The physiological data we have presented here will be useful in investigating those stimuli in the natural environment to which these butterflies may respond. Lastly, the behavioral and ecological significance of this physiological data needs further investigation. Even with modeling data, we will need to verify our predictions with behavioral experiments. Comparison of these species' eyes with those of others can help to expand upon our knowledge of how a prey's sensory system contributes to the generation and maintenance of biodiversity.

Acknowledgments

We thank Omar Ávalos, Francesca Frentiu, Fred Gagnon, Blanca Claudia Hernández, Maita Kuvhenguhwa, Gordon Pratt, Marysol Trujano, and Andrew Warren for assistance with specimen collection, the Costa Rica Entomological Supply for providing pupae, and Maita Kuvhenguhwa and Zachary Johnston for technical support. This work was supported by NSF DEB-1342706 to R.I.H. and DEB-1342759 and IOS-1656260 to A.D.B

Author contributions:

A.D., G.D.B, S.P.M, and A.D.B. designed research; A.D., G.D.B., A.M.M., F.Y., R.I.H, J.P.L, A.G.R.O., A.L.-M., J.L.B. performed research; A.D., G.D.B., F.Y., A.M.M., A.G.R.O., and A.D.B. analyzed data; A.D. and A.D.B. wrote the paper.

References

Aiello A (1984). *Adelpha* (Nymphalidae): Deception on the wing. *Psyche*, 91: 1–45. https://doi.org/10.1155/1984/87930

Arikawa K, Pirih P and Stavenga DG (2009). Rhabdom constriction enhances filtering by the red screening pigment in the eye of the Eastern Pale Clouded yellow butterfly, *Colias erate* (Pieridae). *Journal of Experimental Biology*, 212: 2057–2064. https://doi.org/10.1242/jeb.030692

Beccaloni GW, Viloria AL, Hall SK and Robinson GD (2008). Catalogue of the hostplants of the Neotropical butterflies. Sociedad Entomológica Aragonesa, Monografías Tercer Milenio, Vol. 8 Zaragoza, Spain.

Belušic G, Ilić M, Meglič A, Pirih P (2021). Red-green opponency in the long visual fibre photoreceptors of brushfoot butterflies (Nymphalidae) *Proceedings of the Royal Society B,* 288: 20211560. https://doi.org/10.1098/rspb.2021.1560

Blackiston D, Briscoe AD, and Weiss MR (2011). Color vision and learning in the monarch butterfly, *Danaus plexippus* (Nymphalidae). *Journal of Experimental Biology*, 214: 509–520. https://doi.org/10.1242/jeb.048728

Bray NL, Pimentel H, Melsted P and Pachter L (2016). Near-optimal probabilistic RNA-seq quantification. *Nature Biotechnology*, 34: 525–527. https://doi.org/10.1038/nbt.3519

Briscoe AD (2008). Reconstructing the ancestral butterfly eye: Focus on the opsins. *Journal of Experimental Biology*, 211: 1805–1813. https://doi.org/10.1242/jeb.013045

Briscoe AD and Bernard GD (2005). Eyeshine and spectral tuning of long wavelength-

sensitive rhodopsins: No evidence for red-sensitive photoreceptors among five Nymphalini butterfly species. *Journal of Experimental Biology*, 208: 687–696. https://doi.org/10.1242/jeb.01453

Briscoe AD and Chittka L (2001). The evolution of color vision in insects. *Annual Review of Entomology*, 46: 471–510. https://doi.org/10.1146/annurev.ento.46.1.471

Bybee SM, Yuan F, Ramstetter MD, Llorente-Bousquets J, Reed RD, Osorio D and Briscoe AD (2012). UV photoreceptors and UV-yellow wing pigments in *Heliconius* butterflies allow a color signal to serve both mimicry and intraspecific communication. *The American Naturalist*, 179: 38–51. https://doi.org/10.1086/663192

Chai P (1986). Field observations and feeding experiments on the responses of rufous-tailed jacamars (*Galbula ruficauda*) to free-flying butterflies in a tropical rainforest. *Biological Journal of the Linnean* Society, 29: 161-189.

Cronin TW, Johnsen S, Marshall NJ and Warrant EJ (2014). *Visual Ecology*. Princeton University Press.

Dalbosco Dell'Aglio D, Troscianko J, Mcmillan WO, Stevens M and Jiggins CD (2018). The appearance of mimetic *Heliconius* butterflies to predators and conspecifics. Evolution, 72: 2156–2166. https://doi.org/10.1111/evo.13583

Darst CR and Cummings ME (2006). Predator learning favours mimicry of a less-toxic model in poison frogs. *Nature*, 440: 208–211. https://doi.org/10.1038/nature04297

Dion E, Pui LX, Weber K and Monteiro A (2020). Early-exposure to new sex pheromone

blends alters mate preference in female butterflies and in their offspring. *Nature Communications*, 11:53. https://doi.org/10.1038/s41467-019-13801-2

Ebel ER, DaCosta JM, Sorenson MD, Hill RI, Briscoe AD, Willmott KR and Mullen SP (2015). Rapid diversification associated with ecological specialization in Neotropical *Adelpha* butterflies. *Molecular Ecology*, 24: 2392–2405. https://doi.org/10.1111/mec.13168

Edgar RC (2004). MUSCLE: Multiple sequence alignment with high accuracy and high throughput. *Nucleic Acids Research*, 32:1792–1797. https://doi.org/10.1093/nar/gkh340

Feuda R, Marlétaz F, Bentley MA and Holland PWH (2016). Conservation, duplication, and divergence of five opsin genes in insect evolution. *Genome Biology and Evolution*, 8:579–587. https://doi.org/10.1093/gbe/evw015

Finkbeiner SD and Briscoe AD (2021). True UV color vision in a female butterfly with two UV opsins. *Journal of Experimental Biology*, 224:jeb242802. https://doi.org/10.1242/jeb.242802

Finkbeiner SD, Briscoe AD and Mullen SP (2017a). Complex dynamics underlie the evolution of imperfect wing pattern convergence in butterflies. *Evolution*, 71: 949–959. https://doi.org/10.1111/evo.13165

Finkbeiner SD, Fishman DA, Osorio D and Briscoe AD (2017b). Ultraviolet and yellow reflectance but not fluorescence is important for visual discrimination of conspecifics by *Heliconius erato*. *Journal of Experimental Biology*, 220:1267–1276. https://doi.org/10.1242/jeb.153593

Finkbeiner SD, Salazar PA, Nogales S, Rush CE, Briscoe AD, Hill RI, Kronforst MR,

Willmott KR and Mullen SP (2018). Frequency dependence shapes the adaptive landscape of imperfect Batesian mimicry. *Proceedings of the Royal Society B*, 285: https://doi.org/10.1098/rspb.2017.2786

Frentiu FD and Briscoe AD (2008). A butterfly eye's view of birds. *Bioessays,* 30: 11-12.

Frentiu FD, Bernard GD, Cuevas CI, Sison-Mangus MP, Prudic KL and Briscoe AD (2007a). Adaptive evolution of color vision as seen through the eyes of butterflies. *Proceedings of the National Academy of Sciences U.S.A.*, 104(Supplement 1): 8634–8640. https://doi.org/10.1073/pnas.0701447104

Frentiu FD, Bernard GD, Sison-Mangus MP, Van Zandt Brower A and Briscoe AD (2007b). Gene duplication is an evolutionary mechanism for expanding spectral diversity in the long-wavelength photopigments of butterflies. *Molecular Biology and Evolution*, 24: 2016–2028. https://doi.org/10.1093/molbev/msm132

Frentiu FD, Yuan F, Savage WK, Bernard GD, Mullen SP and Briscoe AD (2015). Opsin clines in butterflies suggest novel roles for insect photopigments. *Molecular Biology and Evolution*, 32: 368–379. https://doi.org/10.1093/molbev/msu304

Gao F, Chen C, Arab DA, Du Z, He Y and Ho SYW (2019). EasyCodeML: A visual tool for analysis of selection using CodeML. *Ecology and Evolution*, 9:3891–3898. https://doi.org/10.1002/ece3.5015

Gibson DO (1974). Batesian mimicry without distastefulness? *Nature*, 250: 77–79. https://doi.org/10.1038/250077a0

Grabherr MG, Haas BJ, Yassour M, Levin JZ, Thompson DA, Amit I, Adiconis X, Fan L, Raychowdhury R, Zeng Q, Chen Z, Mauceli E, Hacohen N, Gnirke A, Rhind N, di Palma F, Birren BW, Nusbaum C, Lindblad-Toh K, … Regev A (2011). Full-

length transcriptome assembly from RNA-Seq data without a reference genome. *Nature Biotechnology*, 29: 644–652. https://doi.org/10.1038/nbt.1883

Haas BJ, Papanicolaou A, Yassour M, Grabherr M, Blood PD, Bowden J, Couger MB, Eccles D, Li B, Lieber M, MacManes MD, Ott M, Orvis J, Pochet N, Strozzi F, Weeks N, Westerman R, William T, Dewey CN, … Regev, A. (2013). *De novo* transcript sequence reconstruction from RNA-seq using the Trinity platform for reference generation and analysis. *Nature Protocols*, 8: 1494–1512. https://doi.org/10.1038/nprot.2013.084

Hill RI and Mullen SP (2019). Adult feeding as a potential mechanism for unprofitability in Neotropical *Adelpha* (Limenitidini, Limenitidinae, Nymphalidae). *Journal of the Lepidopterists' Society*, 73: 66. https://doi.org/10.18473/lepi.73i1.a11

Kelber A, Vorobyev M and Osorio D (2003). Animal colour vision—Behavioural tests and physiological concepts. *Biological Reviews,* 78:81–118. https://doi.org/10.1017/S1464793102005985

Kinoshita M, Takahashi Y and Arikawa K (2012). Simultaneous brightness contrast of foraging *Papilio* butterflies. *Proceedings of the Royal Society B: Biological Sciences*, 279: 1911–1918. https://doi.org/10.1098/rspb.2011.2396

Koshitaka H, Kinoshita M, Vorobyev M and Arikawa K (2008). Tetrachromacy in a butterfly that has eight varieties of spectral receptors. *Proceedings of the Royal Society B: Biological Sciences*, 275: 947–954. https://doi.org/10.1098/rspb.2007.1614

Kram YA, Mantey S and Corbo JC (2010). Avian cone photoreceptors tile the retina as five independent, self-organizing mosaics. *PLoS One*, 5:e8992.

https://doi.org/10.1371/journal.pone.0008992

Kramer VR, Reiter KE and Lehnert MS (2018). Proboscis morphology suggests reduced feeding abilities of hybrid *Limenitis* butterflies (Lepidoptera: Nymphalidae). *Biological Journal of the Linnean Society*, 125: 535–546. https://doi.org/10.1093/biolinnean/bly132

Kristiansen EB, Finkbeiner SD, Hill RH, Prosa L, Mullen SP. 2018. Testing the adaptive hypothesis of Batesian mimicry among hybridizing North American admiral butterflies. *Evolution,* 72: 1436-1448.

Kumar S, Stecher G, Li M, Knyaz C and Tamura K (2018). MEGA X: Molecular evolutionary genetics analysis across computing platforms. *Molecular Biology and Evolution*, 35: 1547–1549. https://doi.org/10.1093/molbev/msy096

Kumar S, Stecher G and Tamura K (2016). MEGA7: Molecular evolutionary genetics analysis version 7.0 for bigger datasets. *Molecular Biology and Evolution*, 33: 1870–1874. https://doi.org/10.1093/molbev/msw054

Kuwalekar M, Dechmukh R, Baral S, Padvi A, Kunte K (2022) Duplication and sub-functionalization characterize diversification of opsin genes in the Lepodoptera. *bioRxiv,* https://doi.org/10.1101/2022.10.31.514481

Lederer G (1960). Verhaltensweisen der Imagines und der Entwicklungsstadien von *Limenitis camilla camilla* L. (Lep. Nymphalidae). *Z. Tierpsychologie,* 1715: 521–546.

Liénard MA, GD Bernard, A Allen, J-M Lassance, S Song, R Rabideau Childers, N Yu, D Ye, A Stephenson, WA Valencia-Montoya, S Salzman, MRL Whitaker, M Calonje, F Zhang, NE Pierce (2021). The evolution of red color vision is linked to

coordinated rhodopsin tuning in lycaenid butterflies. *Proceedings of the National Academy of Sciences, U.S.A.* 118:e2008986118.

Llaurens V, Joron M, Théry M. (2014). Cryptic differences in colour among Müllerian mimics: how can the visual capacities of predators and prey shape the evolution of wing colours? *Journal of Evolutionary Biology,* 27:531-540, https://doi.org/10.1111/jeb.12317

Luis-Martínez A, Ávalos-Hernández O, Trujano-Ortega M, Arellano-Covarrubias A, Vargas-Fernández I, Llorente-Bousquets J (2022). Distribution, diversity, and endemism of Nymphalidae (Lepidoptera: Papilionoidea) in Loxicha Region, Oaxaca, Mexico. *Revista de Biología Tropical*, 70: 363-407. https://doi.org/10.15517/rev.biol.trop..v70i1.48821

Macias-Muñoz A, Rangel Olguin AG and Briscoe AD (2019). Evolution of phototransduction genes in Lepidoptera. *Genome Biology and Evolution*, 11:2107–2124. https://doi.org/10.1093/gbe/evz150

Maia R, Gruson H, Endler JA and White TE (2019). pavo 2: New tools for the spectral and spatial analysis of colour in r. *Methods in Ecology and Evolution*, 10: 1097–1107. https://doi.org/10.1111/2041-210X.13174

Maier EJ and Bowmaker JK (1993). Colour vision in the passeriform bird, *Leiothrix lutea*: Correlation of visual pigment absorbance and oil droplet transmission with spectral sensitivity. *Journal of Comparative Physiology A*, 172:295–301. https://doi.org/10.1007/BF00216611

Mallet J, Jiggins C and McMillan W (1998). Mimicry and warning colour at the boundary between races and species. *Undefined*.

https://www.semanticscholar.org/paper/Mimicry-and-warning-colour-at-the-boundary-between-Mallet-Jiggins/e61e06a41841fe29f2fddc3b72b6d0274bf1d786

Mallet J and Singer MC (1987). Individual selection, kin selection, and the shifting balance in the evolution of warning colours: The evidence from butterflies. *Biological Journal of the Linnean Society*, 32: 337–350. https://doi.org/10.1111/j.1095-8312.1987.tb00435.x

Mavárez J, Salazar CA, Bermingham E, Salcedo C, Jiggins CD and Linares M (2006). Speciation by hybridization in *Heliconius* butterflies. *Nature*, 441: 868–871. https://doi.org/10.1038/nature04738

McClure M, Clerc C, Desbois C, Meichanetzoglou A, Cau M, Bastin-Héline L, Bacigalupo J, Houssin C, Pinna C, Nay B, Llaurens V, Berthier S, Andraud C, Gomez, EM (2019). Why has transparency evolved in aposematic butterflies? Insights from the largest radiation of aposematic butterflies, the Ithomiini. *Proceedings of the Royal Society B,* 286: 20182769, https://doi.org/10.1098/rspb.2018.2769

McCulloch KJ, Osorio D and Briscoe AD (2016). Sexual dimorphism in the compound eye of *Heliconius erato*: A nymphalid butterfly with at least five spectral classes of photoreceptor. *Journal of Experimental Biology*, 219: 2377–2387. https://doi.org/10.1242/jeb.136523

Meneses-Giorgi MA and Cadena CD (2021). Plumage convergence resulting from social mimicry in birds? A tetrachromatic view. *Animal Behaviour*, 180: 337–361. https://doi.org/10.1016/j.anbehav.2021.08.018

Min XJ, Butler G, Storms R and Tsang A (2005). OrfPredictor: Predicting protein-coding regions in EST-derived sequences. *Nucleic Acids Research*, 33(Web Server issue), W677-80. https://doi.org/10.1093/nar/gki394

Montero SV. 2018. Aplicación de modelos de nicho ecológico para la identificación potential de procesos de especiación críptica en *Adelpha basiloides* (Lepidoptera: Nymphalidae) en el territorio de Costa Rica. *Gaudeamus,* 10:1-16.

Mulhair PO, Crowley L, Boyes DH, Lewis OT, Holland PWH (2023) Opsin gene duplication in Lepidoptera: retrotransposition, sex linkage, and gene expression. *bioRxiv,* https://doi.org/10.1101/2023.08.16.552946

Mullen SP, Savage WK, Wahlberg N and Willmott KR (2011). Rapid diversification and not clade age explains high diversity in neotropical *Adelpha* butterflies. *Proceedings of the Royal Society B*, 278: 1777–1785. https://doi.org/10.1098/rspb.2010.2140

Mullen SP, VanKuren NW, Zhang W, Nallu S, Kristiansen EB, Wuyun Q, Liu K, Hill RI, Briscoe AD, Kronforst MR (2020) Distangling population history and character evolution among hybridizing lineages. *Molecular Biology and Evolution,* 37:1295-1305, https://doi.org/10.1093/molbev/msaa004

Nell CS, Riley P, Burger J, Preson KL, Treseder KK, Kamada D, Moore K, Mooney KA. 2023. Consequences for arthropod community structure for an at-risk insectivorous bird. *PLoS One,* 18: e0281081, https://doi.org/10.1371/journal.pone.0281081.

Olsson P, Lind O and Kelber A (2018). Chromatic and achromatic vision: Parameter choice and limitations for reliable model predictions. *Behavioral Ecology*, 29:

273–282. https://doi.org/10.1093/beheco/arx133

Oprian DD, Molday RS, Kaufman RJ and Khorana HG (1987). Expression of a synthetic bovine rhodopsin gene in monkey kidney cells. *Proceedings of the National Academy of Sciences, U.S.A.*, 84: 8874–8878. https://doi.org/10.1073/pnas.84.24.8874

O'Reilly LJ, Agassiz DJL, Neil TR and Holderied MW (2019). Deaf moths employ acoustic Müllerian mimicry against bats using wingbeat-powered tymbals. *Scientific Reports*, 9:1444. https://doi.org/10.1038/s41598-018-37812-z

Páez E, Valkonen JK, Willmott KR, Matos-Maraví P, Elias M and Mappes J (2021). Hard to catch: Experimental evidence supports evasive mimicry. *Proceedings of the Royal Society B*, 288: 20203052. https://doi.org/10.1098/rspb.2020.3052

Palacios AG, Goldsmith TH and Bernard GD (1996). Sensitivity of cones from a cyprinid fish (*Danio aequipinnatus*) to ultraviolet and visible light. *Visual Neuroscience*, 13:411. https://doi.org/10.1017/S0952523800008099

Peitsch D, Fietz A, Hertel H, de Souza J, Ventura DFand Menzel R (1992). The spectral input systems of hymenopteran insects and their receptor-based colour vision. *Journal of Comparative Physiology A*, 170: 23–40. https://doi.org/10.1007/BF00190398

Pfennig DW, Harcombe WR and Pfennig KS (2001). Frequency-dependent Batesian mimicry. *Nature*, 410: 323–323. https://doi.org/10.1038/35066628

Platt AP and Allen JF (2006). Sperm precedence and competition in doubly-mated *Limenitis arthemis-astyanax* butterflies (Rhopalocera: Nymphalidae). *Annals of the Entomological Society of America*, 94: 654–663.

https://doi.org/10.1603/0013-8746(2001)094[0654:spacid]2.0.co;2

Platt AP and Brower LP(2006). Mimetic versus disruptive coloration in intergrading populations of *Limenitis arthemis* and *astyanax* butterflies. *Evolution*, 22: 699. https://doi.org/10.2307/2406897

Pohl N, Sison-Mangus MP, Yee EN, Liswi SW, Briscoe AD (2009). Impact of duplicate gene copies on phylogenetic analysis and divergence time estimates in butterflies. *BMC Evolutionary Biology,* 9:99 doi:10.1186/1471-2148-9-99

Prudic KL, Shapiro A, Clayton NS (2002). Evaluating a putative mimetic relationship between two butterflies, *Adelpha bredowii* and *Limenitis lorquini. Ecological Entomology,* 27: 68-75, https://doi.org/10.1046/j.0307-6946.2001.00384.x

Prudic KL, Khera S, Sólyom A, Timmermann BN (2007) Isolation, identification, and quantification of potential defensive compounds in the viceroy gutterfly and its larval host–plant, Carolina willow. *Journal of Chemical Ecology* 33: 1149–1159, https://doi.org/10.1007/s10886-007-9282-5

Prudic KL, Warren AD, Llorente-Bousquets J (2008). Molecular and morphological evidence reveals three species within the California sister butterfly, *Adelpha bredowii* (Lepidoptera: Nymphalidae: Limenitidinae). Zootaxa 1819:1-24, https://doi.org/10.11646/zootaxa.1819.1.1

Prudic KL, Timmermann BN, Papaj DR, Ritland DB, Oliver JC (2019) Mimicry in viceroy butterflies is dependent on abundance of the model queen butterfly. *Communication Biology* 2: 68. https://doi.org/10.1038/s42003-019-0303-z

Rosser N, Freitas AVL, Huertas B, Joron M, Lamas G, Mérot C, Simpson F, Willmott KR, Mallet J and Dasmahapatra KK (2019). Cryptic speciation associated with

geographic and ecological divergence in two Amazonian *Heliconius* butterflies. *Zoological Journal of the Linnean Society*, 186: 233–249. https://doi.org/10.1093/zoolinnean/zly046

Rowland HM, Ihalainen E, Lindström L, Mappes J, Speed MP (2007). Co-mimics have a mutualistic relationship despite unequal defences. *Nature,* 448: 64-67, https://doi.org/10.1038/nature05899

Rush CE, Freitas AVL, Magaldi L, Willmott KR, Hill RI. (2023). One generalist or several specialists? Comparative analysis of the polyphagous butterfly *Adelpha serpa celerio* and its *serpa*-group relatives. *Zool. Scripta* 52: 475-493

Savage WK and Mullen SP (2009). A single origin of Batesian mimicry among hybridizing populations of admiral butterflies (*Limenitis arthemis*) rejects an evolutionary reversion to the ancestral phenotype. *Proceedings of the Royal Society B: Biological Sciences*, 276: 2557–2565. https://doi.org/10.1098/rspb.2009.0256

Sondhi Y, Ellis EA, Bybee SM, Theobald JC and Kawahara AY (2021). Light environment drives evolution of color vision genes in butterflies and moths. *Communications Biology*, 4: 1–11. https://doi.org/10.1038/s42003-021-01688-z

Spaethe J and Briscoe AD (2005). Molecular characterization and expression of the UV opsin in bumblebees: Three ommatidial subtypes in the retina and a new photoreceptor organ in the lamina. *Journal of Experimental Biology*, 208: 2347–2361. https://doi.org/10.1242/jeb.01634

Stavenga DG (2002). Reflections on colourful ommatidia of butterfly eyes. *Journal of Experimental Biology*, 205: 1077–1085.

Stavenga DG, Kinoshita M, Yang EC and Arikawa K (2001). Retinal regionalization and heterogeneity of butterfly eyes. *Die Naturwissenschaften*, 88: 477–481. https://doi.org/10.1007/s001140100268

Stavenga DG, Smits RP and Hoenders BJ (1993). Simple exponential functions describing the absorbance bands of visual pigment spectra. *Vision Research*, 33: 1011–1017. https://doi.org/10.1016/0042-6989(93)90237-Q

Stobbe N and Schaefer HM (2008). Enhancement of chromatic contrast increases predation risk for striped butterflies. *Proceedings of the Royal Society B*, 275: 1535–1541. https://doi.org/10.1098/rspb.2008.0209

Tamura K and Nei M (1993). Estimation of the number of nucleotide substitutions in the control region of mitochondrial DNA in humans and chimpanzees. *Molecular Biology and Evolution*, 10: 512–526. https://doi.org/10.1093/oxfordjournals.molbev.a040023

Telles FJ, Kelber A and Rodríguez-Gironés MA (2016). Wavelength discrimination in the hummingbird hawkmoth *Macroglossum stellatarum*. *Journal of Experimental Biology*, 219: 553–560. https://doi.org/10.1242/jeb.130484

Thurman TJ and Seymoure BM (2016). A bird's eye view of two mimetic tropical butterflies: coloration matches predator's sensitivity. *Journal of Zoology,* 298: 159-168.

Vorobyev M and Osorio D (1998). Receptor noise as a determinant of colour thresholds. *Proceedings of the Royal Society B*, 265: 351–358. https://doi.org/10.1098/rspb.1998.0302

Vought BW, Salcedo E, Chadwell LV, Britt SG, Birge RR and Knox BE (2000).

Characterization of the primary photointermediates of *Drosophila* rhodopsin. *Biochemistry*, 39: 14128–14137. https://doi.org/10.1021/bi001135k

Wakakuwa M, Stavenga DG, Kurasawa M and Arikawa K (2004). A unique visual pigment expressed in green, red and deep-red receptors in the eye of the small white butterfly, *Pieris rapae crucivora*. *Journal of Experimental Biology*, 207: 2803–2810. https://doi.org/10.1242/jeb.01078

Wakakuwa M, Terakita A, Koyanagi M, Stavenga DG, Shichida Y and Arikawa K (2010). Evolution and mechanism of spectral tuning of blue-absorbing visual pigments in butterflies. *PLoS One*, 5: e15015. https://doi.org/10.1371/journal.pone.0015015

White RH (2003). The retina of *Manduca sexta*: Rhodopsin expression, the mosaic of green-, blue- and UV-sensitive photoreceptors, and regional specialization. *Journal of Experimental Biology*, 206: 3337–3348. https://doi.org/10.1242/jeb.00571

Willmott KR (2003a). The genus *Adelpha*: Its systematics, biology and biogeography (Lepidoptera: Nymphalidae: Limenitidini). Scientific Publishers: Gainesville, Florida.

Willmott KR (2003b). Cladistic analysis of the Neotropical butterfly genus *Adelpha* (Lepidoptera: Nymphalidae), with comments on the subtribal classification of Limenitidini. *Systematic Entomology*, 28: 279–322. https://doi.org/10.1046/j.1365-3113.2003.00209.x

Wu L-W, Chiba H, Lees DC, Ohshima Y and Jeng M-L (2019). Unravelling relationships among the shared stripes of sailors: Mitogenomic phylogeny of Limenitidini

butterflies (Lepidoptera, Nymphalidae, Limenitidinae), focusing on the genera *Athyma* and *Limenitis*. *Molecular Phylogenetics and Evolution*, 130: 60–66. https://doi.org/10.1016/J.YMPEV.2018.09.020

Yang Z (2007). PAML 4: Phylogenetic analysis by maximum likelihood. *Molecular Biology and Evolution*, 24:1586–1591. https://doi.org/10.1093/molbev/msm088

Yang Z and Nielsen R (2002). Codon-substitution models for detecting molecular adaptation at individual sites along specific lineages. *Molecular Biology and Evolution*, 19: 908–917. https://doi.org/10.1093/oxfordjournals.molbev.a004148

Yang Z, Nielsen R, Goldman N and Pedersen AM (2000). Codon-substitution models for heterogeneous selection pressure at amino acid sites. *Genetics*, 155: 431–449. https://doi.org/10.1093/genetics/155.1.431

Zaccardi G, Kelber A., Sison-Mangus MP, Briscoe AD (2006). Color discrimination in the red range with only one long-wavelength sensitive opsin. *Journal of Experimental Biology*, 209:1944–1955. https://doi.org/10.1242/jeb.02207